



# Altered White Matter Integrity in Human Immunodeficiency Virus-Associated Neurocognitive Disorder: A Tract-Based Spatial Statistics Study

Se Won Oh, MD<sup>1</sup>, Na-Young Shin, MD<sup>2</sup>, Jun Yong Choi, MD, PhD<sup>3</sup>, Seung-Koo Lee, MD, PhD<sup>4</sup>, Mi Rim Bang, MS<sup>2</sup>

<sup>1</sup>Department of Radiology, Soonchunhyang University Cheonan Hospital, Cheonan 31151, Korea; <sup>2</sup>Department of Radiology, College of Medicine, The Catholic University of Korea, Seoul 06591, Korea; <sup>3</sup>Department of Internal Medicine and AIDS Research Institute, Yonsei University College of Medicine, Seoul 03722, Korea; <sup>4</sup>Department of Radiology, Research Institute of Radiological Science, Yonsei University College of Medicine, Seoul 03722, Korea

**Objective:** Human immunodeficiency virus (HIV) infection has been known to damage the microstructural integrity of white matter (WM). However, only a few studies have assessed the brain regions in HIV-associated neurocognitive disorders (HAND) with diffusion tensor imaging (DTI). Therefore, we sought to compare the DTI data between HIV patients with and without HAND using tract-based spatial statistics (TBSS).

**Materials and Methods:** Twenty-two HIV-infected patients (10 with HAND and 12 without HAND) and 11 healthy controls (HC) were enrolled in this study. A whole-brain analysis of fractional anisotropy (FA), mean diffusivity (MD), radial diffusivity (RD), and axial diffusivity was performed with TBSS and a subsequent 20 tract-specific region-of-interest (ROI)-based analysis to localize and compare altered WM integrity in all group contrasts.

**Results:** Compared with HC, patients with HAND showed decreased FA in the right frontoparietal WM including the upper corticospinal tract (CST) and increased MD and RD in the bilateral frontoparietal WM, corpus callosum, bilateral CSTs and bilateral cerebellar peduncles. The DTI values did not significantly differ between HIV patients with and without HAND or between HIV patients without HAND and HC. In the ROI-based analysis, decreased FA was observed in the right superior longitudinal fasciculus and was significantly correlated with decreased information processing speed, memory, executive function, and fine motor function in HIV patients.

**Conclusion:** These results suggest that altered integrity of the frontoparietal WM contributes to cognitive dysfunction in HIV patients.

**Keywords:** Human immunodeficiency virus; HIV; HIV-associated neurocognitive disorders (HAND); Diffusion tensor imaging; TBSS

Received April 3, 2017; accepted after revision September 28, 2017. This study was supported funding by the Basic Science Research Program through the National Research Foundation of Korea (NRF) funded by the Ministry of Education, Science and Technology (NRF-2013R1A1A2005412) and the Soonchunhyang University Research Fund.

**Corresponding author:** Na-Young Shin, MD, Department of Radiology, College of Medicine, The Catholic University of Korea, 222 Banpo-daero, Seocho-gu, Seoul 06591, Korea.

• Tel: (822) 2558-1443 • Fax: (822) 599-6771

• E-mail: nyshin@catholic.ac.kr

This is an Open Access article distributed under the terms of the Creative Commons Attribution Non-Commercial License (<http://creativecommons.org/licenses/by-nc/4.0>) which permits unrestricted non-commercial use, distribution, and reproduction in any medium, provided the original work is properly cited.

## INTRODUCTION

Human immunodeficiency virus (HIV) infection, previously known as a life-limiting disease, is now regarded as a chronic, manageable disease after the development of combination antiretroviral treatment (cART) (1). With this advance in treatment, the number of possibly fatal opportunistic infections has been dramatically reduced along with cases of severe dementia secondary to HIV infection. However, in patients who undergo long-term treatment, milder forms of HIV-associated neurocognitive disorders (HAND) are still detected (2). The prevalence of HAND is substantial in the Korean (26.3%) as well as the

Western (16–52%) populations even in patients with the virus under successful control, and this cognitive decline impairs the daily functioning of HIV patients (3-5).

Diagnosing HAND is often challenging during the typical outpatient visit and requires complicated neuropsychological (NP) tests (6). However, these NP tests are tedious and may not be confirmative in patients with physical or sensory disability, or illiteracy (7, 8).

While conventional MRI cannot satisfactorily assess HAND in early diagnosis (9, 10), early assessment might be possible with diffusion tensor imaging (DTI). DTI evaluates water diffusion in the white matter (WM) of the brain and shows brain integrity based on indices such as fractional anisotropy (FA), mean diffusivity (MD), axial diffusivity (AD), and radial diffusivity (RD). It is widely used to detect microstructural abnormalities of WM in various types of disease including HIV infection (9, 11). In previously published studies, HIV-infected patients showed decreased FA and increased MD and RD values in various portions of WM including the corpus callosum, hippocampi, deep and periventricular WM, and striatocapsular area (9, 12). However, few studies used DTI to compare HAND in HIV-infected patients with those without cognitive impairment. We hypothesized that differences in WM integrity between these two groups may contribute to our understanding of the underlying pathophysiology of HAND and facilitate the development of appropriate diagnostic tools.

Therefore, we investigated the integrity of WM in patients with HAND by comparing DTI values with HIV-infected patients with intact cognition (HIV-IC) and healthy controls (HC). We processed DTI data using tract-based spatial statistics (TBSS) to identify microstructural changes in the WM tracts. An additional region-of-interest (ROI) analysis was performed using masks that were extracted from the TBSS analysis. We also performed a correlation analysis between mean DTI values calculated from the ROIs with NP test results to correlate microstructural changes in WM with neurocognitive function in HIV patients.

## MATERIALS AND METHODS

### Subjects

This prospective study was approved by the Institutional Review Board and informed consent was obtained from all patients and HC. Between December 2012 and September 2014, 22 HIV patients (10 with HAND and 12 without HAND [HIV-IC]) underwent DTI and standardized NP tests

(4) within a one-month interval. Patients with comorbid conditions that could influence cognitive status and/or daily functioning were excluded, according to the criteria described elsewhere (4, 6). We also recruited 11 age- and sex-matched HC without objective cognitive impairment.

### Assessment of Cognitive Status

To assess the cognitive status, all the HIV patients underwent NP tests designed to represent six cognitive domains: 1) speed of information processing (Korean version of Wechsler Adult Intelligence Scale [K-WAIS] digit symbol subtest and trail making test part A [TMT A]); 2) memory including learning and recall (Korean version of auditory verbal learning test [K-AVLT] and complex figure test); 3) abstraction/executive function (Wisconsin Card Sorting Test [WCST], K-WAIS similarity subtest, and trail making test part B [TMT B]); 4) attention/working memory (K-WAIS digit span subtest); 5) sensory perception/motor skills (Grooved Pegboard Test); and 6) verbal/language (K-WAIS vocabulary subtest). The scores of TMT A, TMT B, and the Grooved Pegboard Test represent time in seconds spent to complete a given task and higher scores denote poor performance. The scores of the other tests are represented as either a standard score or age-scaled score and higher scores denote better performance. Cognitive status was classified as impaired when the scores were greater than 1 standard deviation below the demographically adjusted normative mean from published results with HIV-negative subjects (13-17). Frascati criteria (6) were used in the outpatient clinic to clinically diagnose HAND.

### Statistical Analyses for Demographics and NP Test Results

Age and years of education were compared between the three groups using ANOVA and the Kruskal-Wallis test. The two-sample *t* test and Mann-Whitney test were performed to compare NP test results between the HAND and HIV-IC groups. All the statistical analyses were performed using SPSS version 20.0 (IBM Corp., Armonk, NY, USA). *P* < 0.05 was considered statistically significant.

### Image Acquisition

All the scans were acquired using a 3T scanner (MAGNETOM Trio Tim, Siemens, Erlangen, Germany) with a 32-channel head coil. Head motion was minimized with restraining foam pads provided by the manufacturer. An axial diffusion tensor single-shot echo-planar imaging acquisition was

performed with the following parameters: 60 non-collinear, non-coplanar directions using  $b = 3000 \text{ s/mm}^2$  with 7 baseline images without diffusion weighting; number of excitation = 1; field of view = 230 mm; echo time = 109 ms; repetition time = 10000 ms; flip angle =  $90^\circ$ ; slice thickness = 2.3 mm; in-plane resolution =  $2.3 \times 2.3 \text{ mm}^2$ ; and 72 axial slices. Total acquisition time was 11 minutes 40 seconds.

### Post-Processing of DTI Data and TBSS Analysis

All the DTI data were processed using the Functional Magnetic Resonance Imaging of the Brain (FMRIB) Software Library (FSL) program (<http://www.fmrib.ox.ac.uk/fsl/>). Motion artifacts and eddy current distortions were first corrected by normalization of each directional volume to the non-diffusion-weighted volume ( $b_0$ ) using the FMRIB Linear Image Registration Tool with 6 degrees of freedom. The diffusion tensor was calculated using simple least-squares fit of the tensor model, and FA, MD, AD, and RD maps were computed for each voxel using standard methods for the DTIFIT program in FSL. All the FA images were aligned to the standard FMRIB58\_FA template, which was provided by the FSL program using a nonlinear registration algorithm implemented in the TBSS package. The FA images were then averaged to create a mean FA skeleton. Each subject's aligned FA images were projected onto this skeleton by filling each voxel on the skeleton with the maximum FA values from a plane perpendicular to the local skeleton structure (18). To exclude voxels of adjacent gray matter or cerebrospinal fluid, a threshold FA value of 0.2 was chosen. The MD, AD, and RD maps were also processed with the same method used for the FA maps by applying the nonlinear registration algorithm and projecting them onto the mean FA skeleton. Voxel-wise statistical analysis of individual skeleton images was performed using nonparametric permutation-based two-sample  $t$  tests to compare the DTI values for each group pair. The null distribution was constructed over 5000 permutations.

The threshold-free cluster enhancement approach with two-dimensional parameter settings was used for control over the multiple comparison correction. All the results derived from TBSS analysis were considered significant with a family-wise error-corrected  $p < 0.05$ . To identify WM tracts, two WM atlases within FSL (<http://fsl.fmrib.ox.ac.uk/fsl/data/atlas-descriptions.html>), the Johns Hopkins University (JHU) WM tractography atlas and the International Consortium of Brain Mapping-DTI WM labels atlas, were used.

### ROI-Based Analysis of DTI Values and Correlation Analysis with NP Tests

The group comparison results were significant only between the HAND and control groups on TBSS analysis, which might be attributed to the relatively small number of subjects in our cohort. Therefore, we performed an ROI-based analysis to define group differences between the HAND and HIV-IC groups, our main study goal. In this analysis, we defined masks on areas which revealed significantly different diffusion measures (FA, MD, and RD) between the HAND and HC groups. Then, we subdivided WM into 20 tracts identified by the JHU WM tractography atlas (Supplementary Fig. 1 in the online-only Data Supplement), which is comprised of the left/right (L/R) anterior thalamic radiation (ATR), L/R corticospinal tract (CST), L/R cingulum (cingulate gyrus), L/R cingulum (hippocampus), forceps major, forceps minor, L/R inferior fronto-occipital fasciculus (IFOF), L/R inferior longitudinal fasciculus (ILF), L/R superior longitudinal fasciculus (SLF), L/R uncinate fasciculus, and L/R SLF temporal part using the semi-automated method. Subsequently, we created tract-specific masks with brain regions that showed significant differences between the HAND and HC groups on TBSS analysis overlapping with the ROI of each atlas. As a result, we divided the FA masks into the right CST, right SLF, and right SLF temporal part; MD masks into bilateral ATR, bilateral cingulum (cingulate gyrus), bilateral CST, forceps major and minor, bilateral IFOF, bilateral ILF, bilateral SLF, bilateral SLF temporal part, and left uncinate fasciculus; and RD masks into 19 parts except for the cingulum (hippocampus). We extracted the mean DTI values from each tract-specific ROI projected onto each subject's skeletonized map and compared the mean values between groups using ANOVA, a post-hoc analysis with the two-sample  $t$  test and Kruskal-Wallis test, and a post-hoc analysis with the Mann-Whitney test applying a corrected  $p$  value by the Bonferroni method according to the results of the normality test, respectively. Additionally, we performed trend analyses of DTI values in the ROI between the groups using the Jonckheere-Terpstra test under the hypothesis that HC, HIV-IC, and HAND were all components of a single disease spectrum (with altered WM representing the most severe parameter in the HAND group). To define the WM tract associated with the cognitive decline in HIV patients, we performed a correlation analysis between DTI values of a particular WM tract and NP test scores showing significant differences between the HAND and HIV-IC groups using Pearson's and

Spearman's tests for normally and non-normally distributed data, respectively. All statistical analyses were performed using SPSS version 20.0 (IBM Corp.).

## RESULTS

### Demographics

All the subjects enrolled in this study were male, without any significant differences in age ( $53.0 \pm 2.3$  years,  $52.5 \pm 2.0$  years, and  $56.0 \pm 2.6$  years;  $p = 0.699$ ) or years of education ( $12.4 \pm 0.4$  years,  $12.8 \pm 1.0$  years, and  $13.2 \pm 1.3$  years;  $p = 0.958$ ) between the HC, HIV-IC, and HAND groups. All patients were on stable highly active anti-retroviral therapy and had CD4 > 200 cells/mL and viral load < 20 copies/mL except for one patient in the HAND group who had a viral load of 52.2 copies/mL. Although the HAND group required a longer mean time to complete TMT A ( $p = 0.032$ ), only one HAND patient met the criteria of impaired information processing speed. On the other hand, compared with the HIV-IC group, the HAND group showed cognitive

dysfunction associated with memory including learning and recall ( $p = 0.010$ ), abstraction/executive function ( $p = 0.002$ ), and sensory perception or motor skills ( $p = 0.008$ ). Patients in the HAND group had lower memory scores on K-AVLT sub-tests, lower executive function in WCST and TMT B, and higher motor dysfunction in the Grooved Pegboard Test than patients in the HIV-IC group. The NP test results are briefly summarized in Table 1.

### TBSS Results

Compared with the HC group, the HAND group showed decreased FA in the right corona radiata including CST (Fig. 1) and increased MD in the bilateral superior and posterior corona radiata, right anterior corona radiata, bilateral SLF and ILF, body and splenium of corpus callosum, bilateral posterior limbs and retrolenticular parts of internal capsules, bilateral posterior thalamic radiations, bilateral cerebral peduncles, bilateral sagittal striata, and bilateral cerebellar peduncles and medial lemnisci (Fig. 2). For RD, the HAND group showed increased values in the bilateral

**Table 1. Neuropsychological Status of HIV-IC and HAND**

|   | HIV-IC (n = 12) | HAND (n = 10) | P      |
|---|-----------------|---------------|--------|
| Speed of information processing (preserved/impaired)      | 12/0            | 9/1           | 0.455  |
| K-WAIS digit symbol subtest, ASS <sup>†</sup>             | 13.3 ± 0.4      | 12.5 ± 0.7    | 0.628  |
| TMT A, s  | 27.5 ± 2.4      | 39.6 ± 4.5    | 0.032* |
| Memory including learning and recall (preserved/impaired) | 12/0            | 5/5           | 0.010* |
| K-AVLT delayed recall, ASS                                | 11.8 ± 0.6      | 7.9 ± 1.2     | 0.008* |
| K-AVLT delayed recognition, ASS                           | 11.8 ± 0.8      | 9.7 ± 1.0     | 0.117  |
| K-AVLT total (Trial 1–5), SS <sup>†</sup>                 | 60.5 ± 6.9      | 47.8 ± 10.8   | 0.006* |
| KCFT copy, ASS <sup>†</sup>                               | 15.5 ± 0.6      | 15.4 ± 0.7    | 1.000  |
| KCFT immediate recall, ASS                                | 14.6 ± 0.7      | 13.1 ± 1.1    | 0.251  |
| KCFT delayed recall, ASS                                  | 14.3 ± 0.8      | 13.2 ± 1.1    | 0.406  |
| Abstraction or executive function (preserved/impaired)    | 11/1            | 2/8           | 0.002* |
| WCST percent conceptual level responses, SS               | 103 ± 4.8       | 82.6 ± 4.6    | 0.006* |
| WCST perseverative errors, SS <sup>†</sup>                | 106.8 ± 5.7     | 87.8 ± 4.1    | 0.080  |
| WCST total number of errors, SS                           | 103.8 ± 4.8     | 81.8 ± 5.1    | 0.005* |
| K-WAIS similarity subtest, ASS                            | 12.7 ± 0.6      | 12.2 ± 0.8    | 0.628  |
| TMT B, s <sup>†</sup>                                     | 88.3 ± 12.2     | 189.7 ± 44.1  | 0.030* |
| Attention or working memory (preserved/impaired)          | 12/0            | 12/0          | N/A    |
| K-WAIS digits span subtest, ASS                           | 13.7 ± 0.8      | 11.9 ± 0.9    | 0.165  |
| Sensory Perception or motor skills (preserved/impaired)   | 10/2            | 2/8           | 0.008* |
| Grooved Pegboard Test, s <sup>†</sup>                     | 63.7 ± 3.1      | 87.7 ± 9.2    | 0.003* |
| Verbal or language (preserved/impaired)                   | 12/0            | 1/9           | 0.455  |
| K-WAIS vocabulary subtest <sup>†</sup>                    | 11.9 ± 0.6      | 11.3 ± 0.9    | 0.346  |

Data are mean values ± standard deviation. \* $p < 0.05$ , <sup>†</sup>Tested using nonparametric method. ASS = age-scaled scores, HAND = HIV-associated neurocognitive disorders, HIV = human immunodeficiency virus, HIV-IC = HIV-infected patients with intact cognition, K-AVLT = Korean version of Auditory Verbal Learning Test, KCFT = age-corrected scores on Korean complex figure test, K-WAIS = Korean version of Wechsler Adult Intelligence Scale, N/A = not applicable, s = seconds, SS = standard scores, TMT A = trail making test part A, TMT B = trail making test part B, WCST = Wisconsin Card Sorting Test

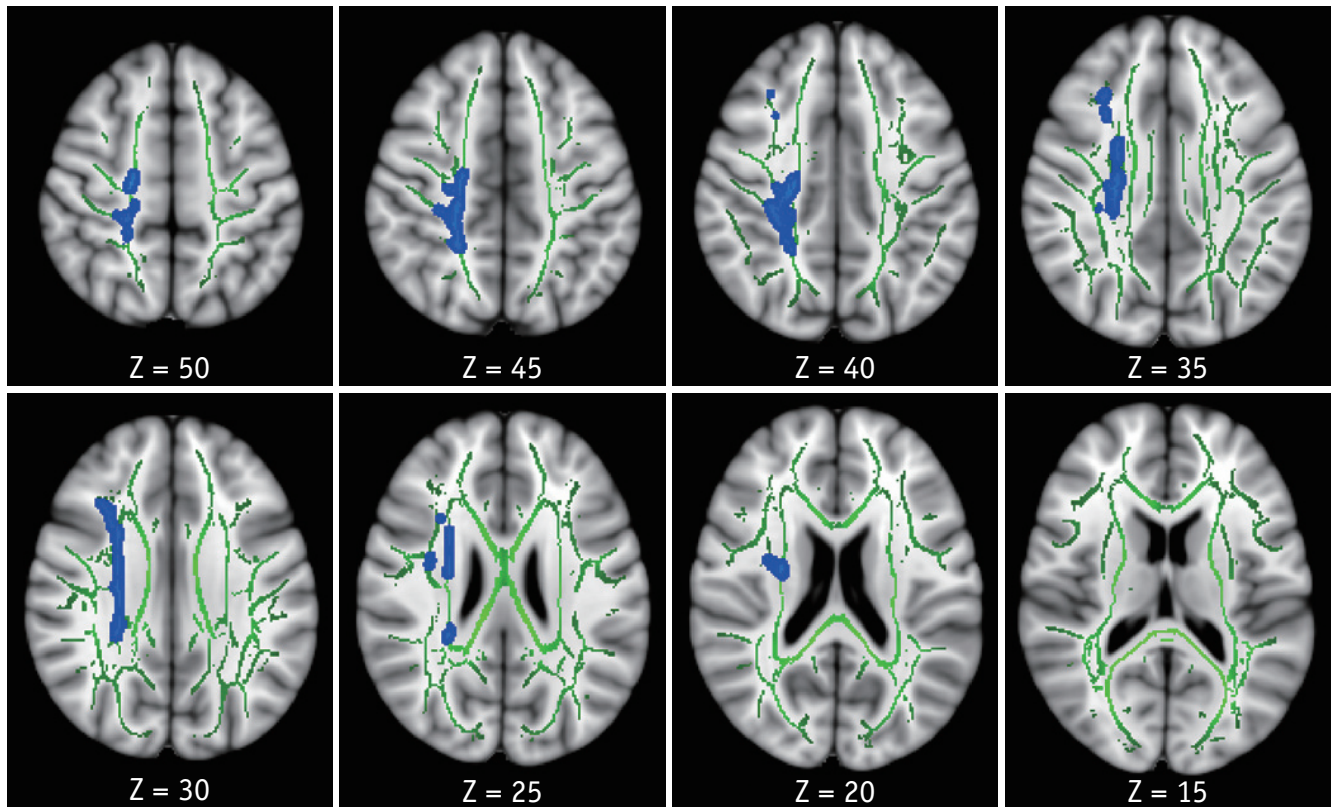


**Fig. 1. TBSS analysis of FA maps.** Areas in sky blue represent brain regions with significant decrease in FA (FWE-corrected  $p < 0.05$ ) in HAND group relative to HC. Results are shown overlaid on Montreal Neurological Institute 152-T1 template and mean FA skeleton (green). Left side of image corresponds to right hemisphere of brain. FA = fractional anisotropy, FWE = family-wise error, HAND = HIV-associated neurocognitive disorders, HC = healthy controls, HIV = human immunodeficiency virus, TBSS = tract-based spatial statistics

corona radiata, bilateral SLF and ILF, corpus callosum, bilateral internal capsule, bilateral thalamic radiations, bilateral superior and middle cerebellar peduncles, and bilateral medial lemnisci (Fig. 3). AD values were not significantly different between the HAND and HC groups. DTI values did not significantly differ between the HAND and HIV-IC groups, nor did they differ between the HIV-IC and HC groups.

#### ROI-Based Analyses of DTI Values between the Groups

Compared with the HIV-IC group, the HAND group showed significantly lower mean FA in the right SLF mask ( $p = 0.008$ ). Although there were no significant differences, the mean MD in the left SLF temporal ( $p = 0.058$ ) masks and the mean RD in the left SLF mask ( $p = 0.059$ ) showed higher values in the HAND group compared with the HIV-IC group. Compared with the HC group, the HIV-IC group showed significantly altered DTI values mainly in CST, ATR, IFOF, and ILF and the HAND group showed altered DTI values in wider areas (Table 2). In the trend analysis, all but the mean MD in the forceps minor and right cingulum (hippocampus)

masks demonstrated significant trends across the groups. All the mean FA values showed an increasing trend from the HC group to the HAND group, while the mean MD and RD values showed a decreasing trend (Fig. 4).

#### Correlation between WM Tract Integrity and Cognitive Function among the HIV Patients

Among the seven NP tests which showed significant differences between the HAND and HIV-IC groups, the K-AVLT total scores and time in seconds required to complete TMT A and B, and the Grooved Pegboard Test showed significant correlation with mean DTI values in tract-specific ROIs showing significant group differences. A lower mean FA value in the right SLF mask was associated with lower performance of TMT A ( $r = -0.425$ ,  $p = 0.049$ ) and B ( $r = -0.455$ ,  $p = 0.038$ ), the K-AVLT test ( $r = 0.564$ ,  $p = 0.006$ ), and the Grooved Pegboard Test ( $r = -0.475$ ,  $p = 0.025$ ) (Fig. 5). Among the mean DTI values in the masks showing different trends between the HAND and HIV-IC groups, a higher MD value in the left SLF temporal part was associated with lower performance of TMT A ( $r = 0.493$ ,  $p = 0.020$ ).

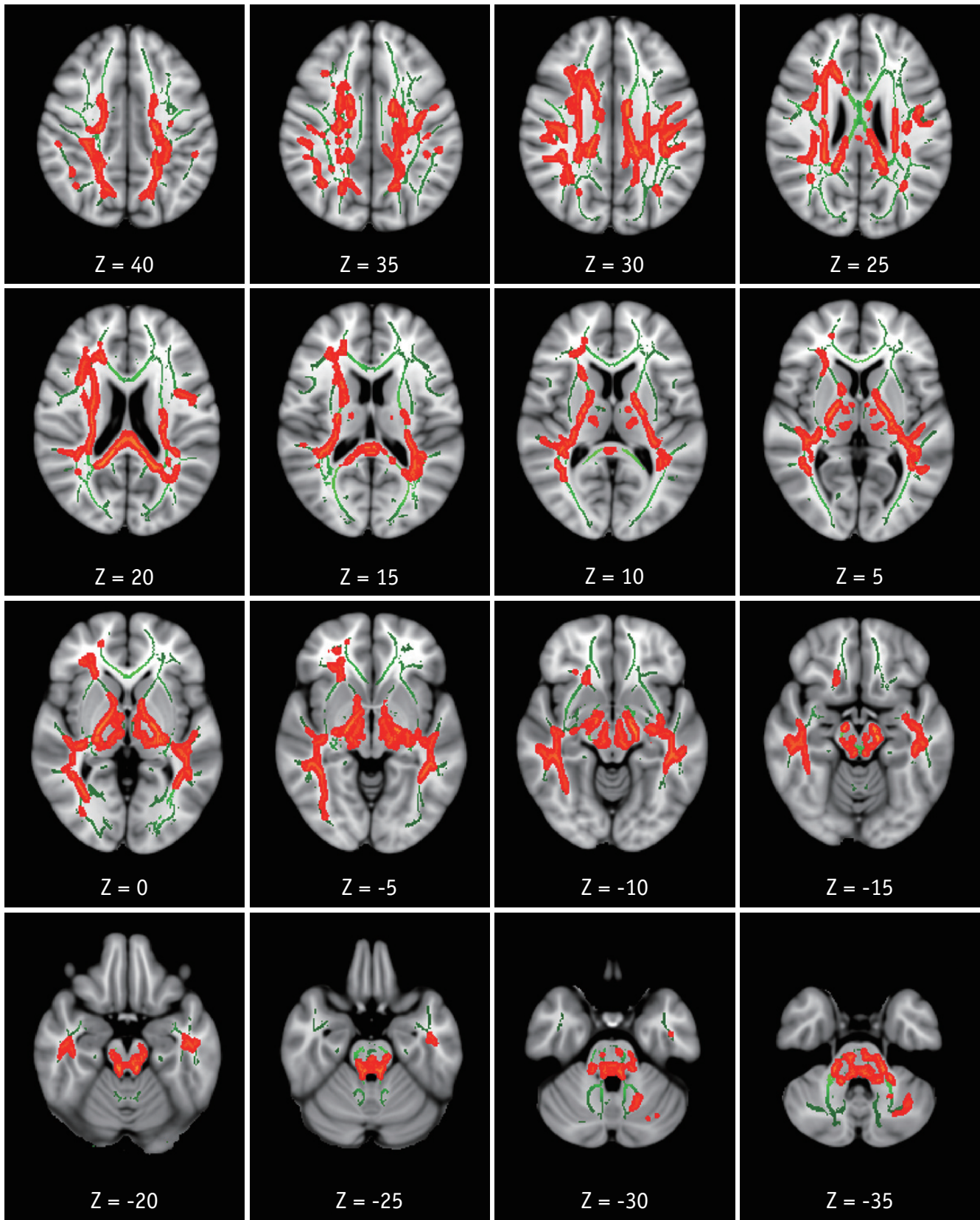


**Fig. 2. TBSS analysis of MD maps.** Areas in orange-red represent brain regions with significant increase in MD (FWE-corrected  $p < 0.05$ ) in HAND group relative to HC. Green represents mean white matter skeleton of all subjects. MD = mean diffusivity

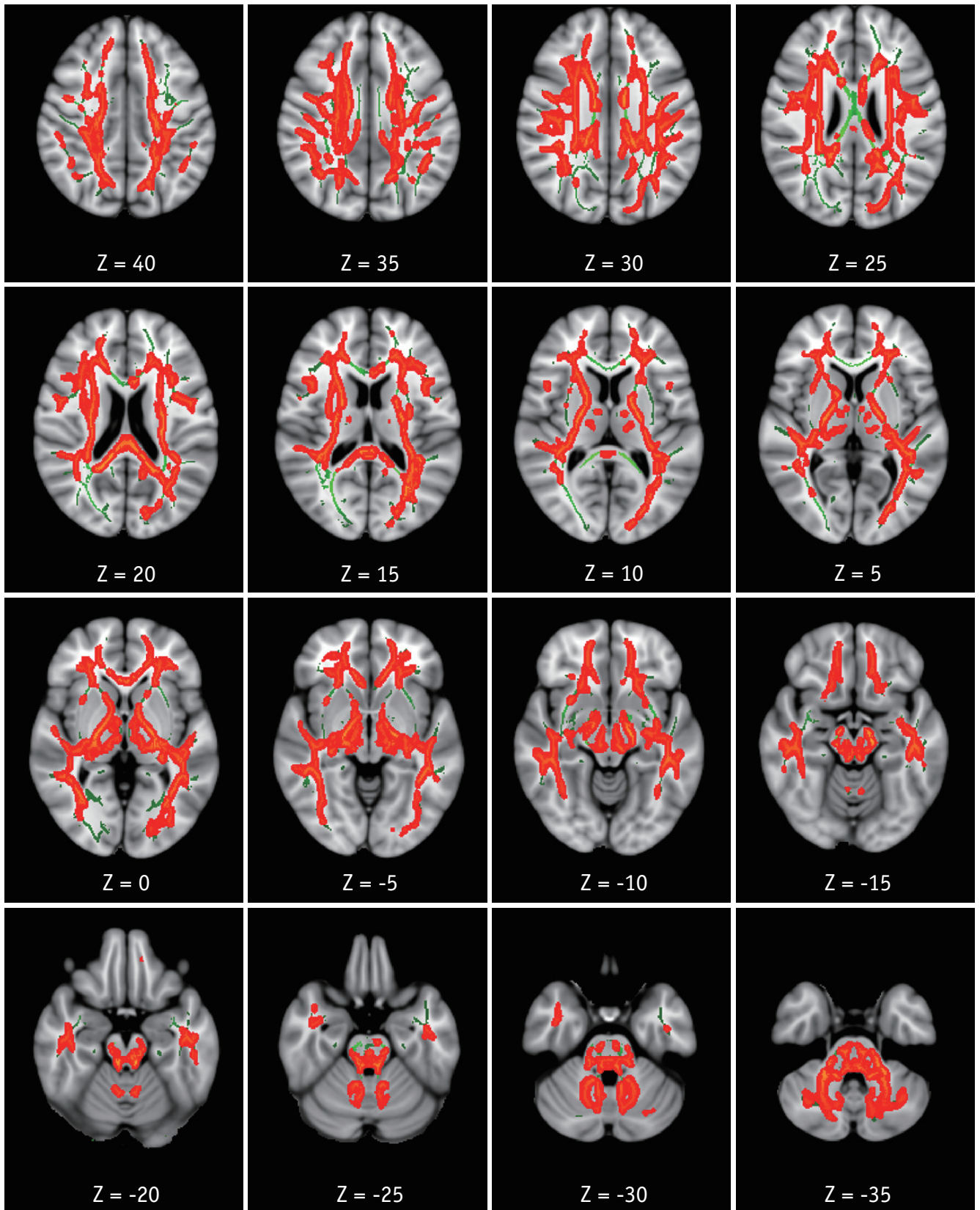


**Fig. 3. TBSS analysis of RD maps.** Areas in orange-red represent brain regions with significant increase in RD (FWE-corrected  $p < 0.05$ ) in HAND group relative to HC. Green represents mean white matter skeleton of all subjects. RD = radial diffusivity

**Table 2. Comparison of Mean DTI Values between Groups in ROI-Based Analysis**

| Mean DTI Values in ROI | HAND (n = 10)     | HIV-IC (n = 12)   | HC (n = 11)       | P <sup>a</sup> | Post-Hoc Analysis |                 |                 |
|------------------------|-------------------|-------------------|-------------------|----------------|-------------------|-----------------|-----------------|
|                        |                   |                   |                   |                | P1 <sup>b</sup>   | P2 <sup>c</sup> | P3 <sup>d</sup> |
| <b>FA</b>              |                   |                   |                   |                |                   |                 |                 |
| CST_R                  | 0.42830 ± 0.02436 | 0.44567 ± 0.02428 | 0.48042 ± 0.02233 | < 0.001*       | 0.290             | < 0.001**       | 0.004**         |
| SLF_R                  | 0.33062 ± 0.03027 | 0.37167 ± 0.02961 | 0.39266 ± 0.02821 | < 0.001*       | 0.008**           | < 0.001**       | 0.291           |
| SLFTP_R                | 0.31225 ± 0.03759 | 0.33253 ± 0.01996 | 0.35941 ± 0.03130 | 0.004*         | 0.372             | 0.003**         | 0.119           |
| <b>MD</b>              |                   |                   |                   |                |                   |                 |                 |
| ATR_L                  | 0.00049 ± 0.00003 | 0.00047 ± 0.00002 | 0.00045 ± 0.00001 | 0.001*         | 0.148             | < 0.001**       | 0.067           |
| ATR_R                  | 0.00048 ± 0.00003 | 0.00047 ± 0.00002 | 0.00044 ± 0.00001 | < 0.001*       | 0.614             | < 0.001**       | 0.005**         |
| CCG_L                  | 0.00054 ± 0.00003 | 0.00053 ± 0.00003 | 0.00050 ± 0.00003 | 0.009*         | 1.000             | 0.010**         | 0.075           |
| CCG_R                  | 0.00050 ± 0.00006 | 0.00050 ± 0.00004 | 0.00046 ± 0.00003 | 0.049*         | 1.000             | 0.091           | 0.109           |
| CST_L                  | 0.00047 ± 0.00002 | 0.00045 ± 0.00001 | 0.00043 ± 0.00001 | < 0.001*       | 0.139             | < 0.001**       | 0.008**         |
| CST_R                  | 0.00046 ± 0.00002 | 0.00045 ± 0.00001 | 0.00043 ± 0.00001 | < 0.001*       | 0.695             | < 0.001**       | 0.003**         |
| FCPM <sup>†</sup>      | 0.00055 ± 0.00005 | 0.00054 ± 0.00003 | 0.00052 ± 0.00003 | 0.041*         | 0.974             | 0.024           | 0.037           |
| FCPm                   | 0.00050 ± 0.00004 | 0.00049 ± 0.00003 | 0.00047 ± 0.00001 | 0.113          | NA                | NA              | NA              |
| IFOF_L <sup>†</sup>    | 0.00056 ± 0.00004 | 0.00054 ± 0.00002 | 0.00051 ± 0.00002 | 0.002*         | 0.203             | 0.001**         | 0.004**         |
| IFOF_R                 | 0.00054 ± 0.00003 | 0.00053 ± 0.00002 | 0.00050 ± 0.00002 | 0.001*         | 0.419             | 0.001**         | 0.042**         |
| ILF_L <sup>†</sup>     | 0.00053 ± 0.00004 | 0.00051 ± 0.00002 | 0.00049 ± 0.00002 | 0.001*         | 0.228             | < 0.001**       | 0.007**         |
| ILF_R                  | 0.00053 ± 0.00003 | 0.00053 ± 0.00002 | 0.00050 ± 0.00002 | 0.001*         | 0.931             | 0.001**         | 0.012**         |
| SLF_L <sup>†</sup>     | 0.00053 ± 0.00003 | 0.00051 ± 0.00003 | 0.00049 ± 0.00002 | 0.001*         | 0.021             | < 0.001**       | 0.069           |
| SLF_R <sup>†</sup>     | 0.00053 ± 0.00003 | 0.00050 ± 0.00003 | 0.00048 ± 0.00002 | 0.002*         | 0.069             | < 0.001**       | 0.051           |
| SLFTP_L                | 0.00053 ± 0.00003 | 0.00051 ± 0.00002 | 0.00049 ± 0.00002 | 0.001*         | 0.058             | < 0.001**       | 0.129           |
| SLFTP_R                | 0.00052 ± 0.00003 | 0.00050 ± 0.00002 | 0.00048 ± 0.00002 | 0.001*         | 0.194             | 0.001**         | 0.065           |
| UF_L                   | 0.00061 ± 0.00004 | 0.00061 ± 0.00003 | 0.00056 ± 0.00004 | 0.005*         | 1.000             | 0.030**         | 0.006**         |
| <b>RD</b>              |                   |                   |                   |                |                   |                 |                 |
| ATR_L                  | 0.00041 ± 0.00003 | 0.00039 ± 0.00002 | 0.00037 ± 0.00001 | 0.002*         | 0.194             | 0.002**         | 0.128           |
| ATR_R                  | 0.00040 ± 0.00003 | 0.00038 ± 0.00002 | 0.00036 ± 0.00001 | 0.001*         | 0.305             | 0.001**         | 0.038**         |
| CCG_L <sup>†</sup>     | 0.00044 ± 0.00004 | 0.00043 ± 0.00003 | 0.00040 ± 0.00003 | 0.014*         | 0.497             | 0.002**         | 0.059           |
| CCG_R                  | 0.00047 ± 0.00006 | 0.00045 ± 0.00004 | 0.00041 ± 0.00005 | 0.026*         | 1.000             | 0.032**         | 0.112           |
| Ch_R                   | 0.00043 ± 0.00004 | 0.00040 ± 0.00004 | 0.00039 ± 0.00003 | 0.131          | NA                | NA              | NA              |
| CST_L                  | 0.00035 ± 0.00002 | 0.00033 ± 0.00002 | 0.00031 ± 0.00001 | < 0.001*       | 0.151             | < 0.001**       | 0.025**         |
| CST_R                  | 0.00034 ± 0.00002 | 0.00033 ± 0.00002 | 0.00030 ± 0.00001 | < 0.001*       | 0.171             | < 0.001**       | 0.006**         |
| FCPM                   | 0.00038 ± 0.00004 | 0.00036 ± 0.00002 | 0.00034 ± 0.00002 | 0.010*         | 0.235             | 0.008**         | 0.386           |
| FCPm                   | 0.00041 ± 0.00003 | 0.00039 ± 0.00003 | 0.00037 ± 0.00002 | 0.027*         | 0.722             | 0.025**         | 0.281           |
| IFOF_L <sup>†</sup>    | 0.00043 ± 0.00003 | 0.00041 ± 0.00003 | 0.00039 ± 0.00002 | 0.006*         | 0.254             | 0.001**         | 0.044           |
| IFOF_R                 | 0.00043 ± 0.00003 | 0.00042 ± 0.00002 | 0.00039 ± 0.00002 | 0.004*         | 0.402             | 0.003**         | 0.101           |
| ILF_L                  | 0.00042 ± 0.00004 | 0.00039 ± 0.00002 | 0.00037 ± 0.00002 | 0.003*         | 0.127             | 0.002**         | 0.276           |
| ILF_R                  | 0.00044 ± 0.00003 | 0.00043 ± 0.00002 | 0.00040 ± 0.00002 | 0.002*         | 0.554             | 0.002**         | 0.039**         |
| SLF_L                  | 0.00043 ± 0.00004 | 0.00040 ± 0.00003 | 0.00038 ± 0.00002 | 0.003*         | 0.059             | 0.001**         | 0.069           |
| SLF_R                  | 0.00043 ± 0.00003 | 0.00041 ± 0.00003 | 0.00039 ± 0.00002 | 0.002*         | 0.124             | 0.001**         | 0.172           |
| SLFTP_L <sup>†</sup>   | 0.00042 ± 0.00004 | 0.00039 ± 0.00003 | 0.00037 ± 0.00002 | 0.007*         | 0.140             | 0.001**         | 0.118           |
| SLFTP_R                | 0.00042 ± 0.00003 | 0.00040 ± 0.00002 | 0.00037 ± 0.00002 | 0.002*         | 0.346             | 0.002**         | 0.080           |
| UF_L                   | 0.00043 ± 0.00003 | 0.00042 ± 0.00003 | 0.00039 ± 0.00002 | 0.021*         | 0.859             | 0.020**         | 0.189           |
| UF_R                   | 0.00044 ± 0.00003 | 0.00043 ± 0.00002 | 0.00041 ± 0.00002 | 0.013*         | 0.993             | 0.013**         | 0.104           |

Data are mean values ± standard deviation. \**p* < 0.05 in 3-group comparison, \*\**p* < 0.05 (parametric tests) or *p* < 0.017 (nonparametric tests) in post-hoc analysis, <sup>†</sup>Tested using nonparametric method. <sup>a</sup>*P* values for comparison among 3 groups, <sup>b</sup>*P* values for comparison between HAND and HIV-IC groups, <sup>c</sup>*P* values for comparison between HAND and HC groups, <sup>d</sup>*P* values comparison between HIV-IC and HC groups. ATR = anterior thalamic radiation, CCG = cingulum (cingulate gyrus), Ch = cingulum (hippocampus), CST = corticospinal tract, DTI = diffusion tensor imaging, FA = fractional anisotropy, FCPM = forceps major, FCPm = forceps minor, HC = healthy controls, IFOF = inferior fronto-occipital fasciculus, ILF = inferior longitudinal fasciculus, L = left, MD = mean diffusivity, R = right, RD = radial diffusivity, ROI = region-of-interest, SLF = superior longitudinal fasciculus, SLFTP = SLF temporal part, UF = uncinata fasciculus



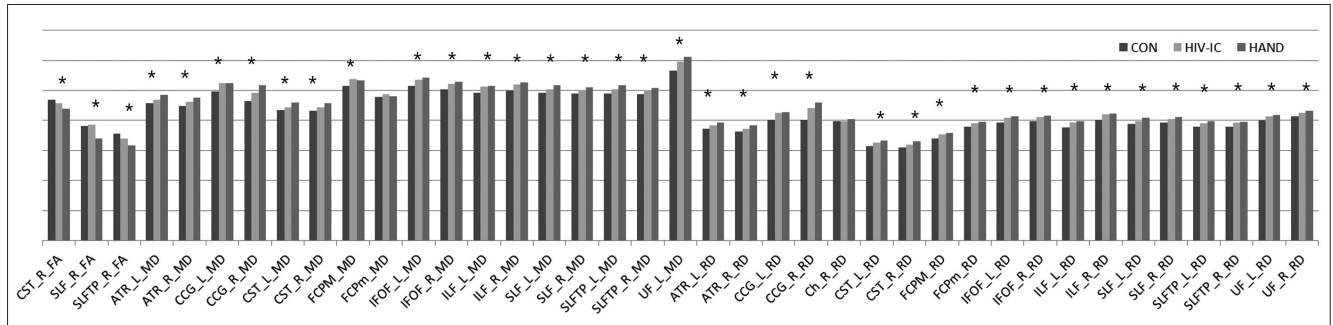


**Fig. 4.** Bar graph representing mean DTI values in JHU WM tractography-based ROIs that were extracted from TBSS results (MD and RD values were multiplied by 1000 for good visibility). \* $p < 0.05$  in trend analyses. ATR = anterior thalamic radiation, CCG = cingulum (cingulate gyrus), Ch = cingulum (hippocampus), CON = healthy controls, CST = corticospinal tract, DTI = diffusion tensor imaging, FCPM = forceps major, FCPm = forceps minor, HIV-IC = HIV-infected patients with intact cognition, IFOF = inferior fronto-occipital fasciculus, ILF = inferior longitudinal fasciculus, JHU = Johns Hopkins University, L = left, R = right, ROI = region-of-interest, SLF = superior longitudinal fasciculus, SLFTP = SLF temporal part, UF = uncinate fasciculus, WM = white matter

## DISCUSSION

Although the exact pathogenesis of HAND is still unclear, recently published neuroimaging studies have discovered widespread microstructural changes in the brain of HIV-infected patients (9). HIV enters the central nervous system via monocytes and perivascular macrophages very early after seroconversion. The virus then replicates and induces neuronal damage mainly by neuroinflammatory mechanisms triggered by infected microglial cells. The inflammation selectively occurs in the dopamine-rich areas of the brain including the prefrontal cortex and frontostriatal network and the resultant neurodegeneration is known to impair cognitive function in HIV-infected patients (2, 19, 20). In a few studies using magnetic resonance (MR) spectroscopy (21, 22) to evaluate cerebral metabolites in the brain *in vivo*, an increased level of inflammatory metabolites was found in the frontal WM and basal ganglia of HIV-infected patients, consistent with previous pathologic studies (23). In addition to neuroinflammation, products of the inflammatory cascade induce oxidative stress in the brain and cerebrospinal fluid of HIV patients (24). Motor neurons are also regarded as targets of neuropathogenesis induced by HIV and their vulnerability to oxidative stress might be one of the plausible mechanisms underlying the injury (25, 26). Therefore, we postulated the incidence of inflammation-induced microstructural alterations mainly in the highly vulnerable frontostriatal and frontoparietal areas as well as the motor tracts.

In this study, using TBSS analysis we found a significantly decreased FA in the right frontoparietal WM and right CST and increased MD in the widespread WM of patients in the HAND group compared with the HC group. The extensive

change in MD was mainly induced by changes in RD rather than AD, similar to previous studies (27-32). RD is known to be related to dys- or demyelination induced by inflammation (33). Therefore, based on previous pathologic studies and MR spectroscopy results, the microstructural changes seen in this study may be, at least in part, attributed to inflammatory demyelination.

The ROI-based analysis showed widespread MD and RD changes already found in the HIV-IC group primarily in the inferior and posterior brain areas as well as the CST compared with the HC group. The HAND group showed additional microstructural alterations in the right frontoparietal WM compared with the HIV-IC group. Our results are in line with previous studies showing cognitively asymptomatic HIV patients carrying microstructural alterations primarily localized in the posterior brain regions and extended abnormalities in the more rostral part of the brain in HAND patients (32). Our results are also in line with studies showing the role of motor cortex in HIV infection regardless of cognitive status, and the association of prefrontal and parietal cortical thinning with cognitive impairment (34, 35). Moreover, most DTI values in tract-specific ROIs showed a significant trend in change starting from the HC group to the HAND group, which suggests that this neural microstructural alteration gradually progresses in HIV-infected patients, a finding also in line with a previously published report (36).

The HAND group in this study showed altered integrity in the superior horizontal part of the right SLF, which was correlated with decreased performance in the NP tests evaluating the speed of information processing, learning memory, executive function and fine motor function. The superior horizontal part of the SLF is a large bundle, which

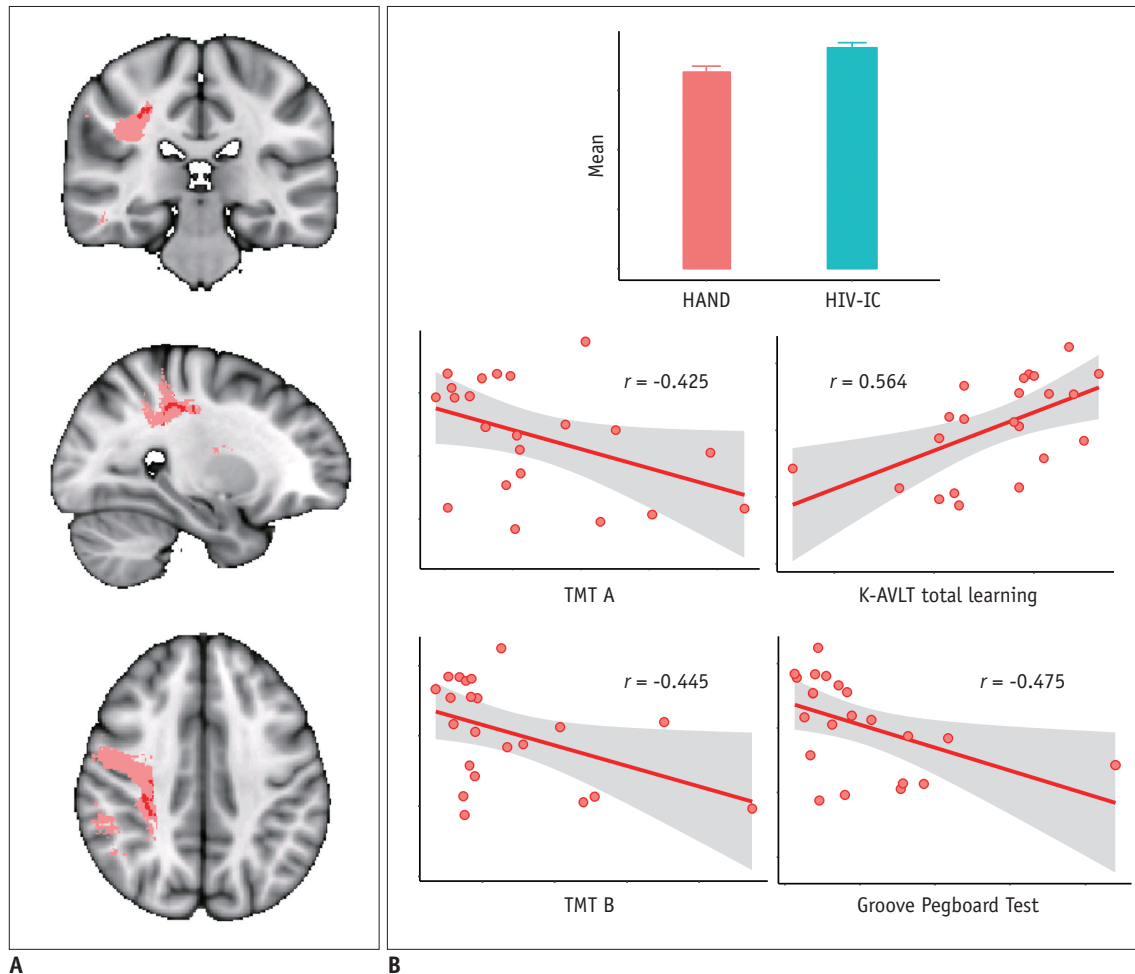


**Fig. 5. Correlation analysis with FA value in right SLF masks and NP test results.**

Region in pink represents right SLF mask in JHU WM tractography atlas. Inside this mask, regions that showed significantly decreased FA between HAND and HIV-IC groups on TBSS analysis are marked in red and was used as mask for ROI (A). Mean FA value in this ROI was correlated with NP test results. Correlation results are shown graphically in (B). K-AVLT = Korean version of Auditory Verbal Learning Test, NP = neuropsychological, TMT A = trail making test part A, TMT B = trail making test part B

connects the superior parietal lobe, the supramarginal gyrus, and the angular gyrus to the ipsilateral frontal cortices (37). Therefore, the SLF mediates the communication and integration of frontal and parietal information and plays an integral role in cognitive function including attention, memory, information processing speed, and language (38). Demyelination of this long fiber may trigger inefficient transmission of neural signals and subsequent cognitive dysfunction (39-41). Interestingly, the integrity of SLF was also associated with lower fine motor function in our study. This result is in agreement with previous studies, which suggest that a loss of compensation of the prefrontal cortex lead to decreased fine motor function in HIV patients with HAND (34, 42).

In TBSS analysis, unlike MD and RD, significantly decreased FA values were localized in the right SLF and CST,

but not in the left hemisphere. In the NP test correlation analyses, a decreased FA in the right SLF was correlated with the cognitive domains. In the additional TBSS analysis with a lower statistical threshold (corrected  $p < 0.07$ , data not shown), the laterality of FA was moderated. While we cannot confirm the factors underlying this laterality, we believe that it may be related to the small number of subjects included in each group of our study. In a few studies investigating cognitive impairment in patients with Parkinson's disease, right-sided dopaminergic depletion was shown to play a greater role in the cognitive decline associated with Parkinson's disease (43-45). As mentioned above, HIV infection also selectively induces inflammatory changes in dopamine-rich structures, suggesting that the right laterality of the microstructural change might be more prominent in HIV patients with HAND.

There are several limitations in this study. First, the small number of subjects in each group lowered the statistical power of the analysis. Second, the cART regimen was not identical in each patient. Previous studies have suggested that nucleoside reverse transcriptase inhibitors can induce neuronal damage. The study patients were all treated with a diverse combination of nucleoside reverse transcriptase inhibitors and other agents (e.g., protease inhibitors, non-nucleoside reverse transcriptase inhibitors and integrase inhibitors). This variation in treatment regimens may have influenced the results.

In conclusion, HIV patients with HAND showed altered microstructures in the bilateral SLF compared with HIV patients without HAND. Additionally, alteration of the bilateral SLF integrity was associated with decreased cognitive function, suggesting a key role in the development of HAND in HIV patients.

## Supplementary Materials

The online-only Data Supplement is available with this article at <https://doi.org/10.3348/kjr.2018.19.3.431>.

## REFERENCES

- Holt JL, Kraft-Terry SD, Chang L. Neuroimaging studies of the aging HIV-1-infected brain. *J Neurovirol* 2012;18:291-302
- Schouten J, Cinque P, Gisslen M, Reiss P, Portegies P. HIV-1 infection and cognitive impairment in the cART era: a review. *AIDS* 2011;25:561-575
- Dore GJ, McDonald A, Li Y, Kaldor JM, Brew BJ; National HIV Surveillance Committee. Marked improvement in survival following AIDS dementia complex in the era of highly active antiretroviral therapy. *AIDS* 2003;17:1539-1545
- Ku NS, Lee Y, Ahn JY, Song JE, Kim MH, Kim SB, et al. HIV-associated neurocognitive disorder in HIV-infected Koreans: the Korean NeuroAIDS Project. *HIV Med* 2014;15:470-477
- Chernoff RA, Martin DJ, Schrock DA, Huy MP. Neuropsychological functioning as a predictor of employment activity in a longitudinal study of HIV-infected adults contemplating workforce reentry. *J Int Neuropsychol Soc* 2010;16:38-48
- Antinori A, Arendt G, Becker JT, Brew BJ, Byrd DA, Cherner M, et al. Updated research nosology for HIV-associated neurocognitive disorders. *Neurology* 2007;69:1789-1799
- Hill-Briggs F, Dial JG, Morere DA, Joyce A. Neuropsychological assessment of persons with physical disability, visual impairment or blindness, and hearing impairment or deafness. *Arch Clin Neuropsychol* 2007;22:389-404
- Ostrosky-Solis F, Ardila A, Rosselli M, Lopez-Arango G, Uriel-Mendoza V. Neuropsychological test performance in illiterate subjects. *Arch Clin Neuropsychol* 1998;13:645-660
- Masters MC, Ances BM. Role of neuroimaging in HIV-associated neurocognitive disorders. *Semin Neurol* 2014;34:89-102
- Karampekios S, Hesselink J. Cerebral infections. *Eur Radiol* 2005;15:485-493
- Sundgren PC, Dong Q, Gómez-Hassan D, Mukherji SK, Maly P, Welsh R. Diffusion tensor imaging of the brain: review of clinical applications. *Neuroradiology* 2004;46:339-350
- Dore GJ, Correll PK, Li Y, Kaldor JM, Cooper DA, Brew BJ. Changes to AIDS dementia complex in the era of highly active antiretroviral therapy. *AIDS* 1999;13:1249-1253
- Heaton RK, Chelune GJ, Talley JL, Kay GG, Curtiss G. *Wisconsin card sorting test manual: revised and expanded*. Odessa, FL: Psychological Assessment Resources, 1993:92-193
- Kim HK. *Handbook of Rey-Kim memory assessment*. Daegu: Neuropsychology Press, 1999:130-148
- Kim MK, Hyun MH. Relationships between Trail Making Test (A, B, B-A, B/A) scores and age, education, comparison of performance head injury patient and psychiatric patient. *Korean J Clin Psychol* 2004;23:353-366
- Lee T. Normative values for the Grooved Pegboard Test in adult. *Phys Ther Korea* 2001;8:87-94
- Yeom TH, Park YS, Oh KJ, Kim JK, Lee YH. *K-WAIS manual*. Seoul: Korea Guidance, 1992:105-119
- Smith SM, Jenkinson M, Johansen-Berg H, Rueckert D, Nichols TE, Mackay CE, et al. Tract-based spatial statistics: voxelwise analysis of multi-subject diffusion data. *Neuroimage* 2006;31:1487-1505
- Purohit V, Rapaka R, Frankenheim J, Avila A, Sorensen R, Rutter J. National Institute on Drug Abuse symposium report: drugs of abuse, dopamine, and HIV-associated neurocognitive disorders/HIV-associated dementia. *J Neurovirol* 2013;19:119-122
- Mediouni S, Marcondes MC, Miller C, McLaughlin JP, Valente ST. The cross-talk of HIV-1 Tat and methamphetamine in HIV-associated neurocognitive disorders. *Front Microbiol* 2015;6:1164
- Lentz MR, Kim WK, Kim H, Soulas C, Lee V, Venna N, et al. Alterations in brain metabolism during the first year of HIV infection. *J Neurovirol* 2011;17:220-229
- Valcour V, Chalermchai T, Sailasuta N, Marovich M, Lerdlum S, Suttichom D, et al. Central nervous system viral invasion and inflammation during acute HIV infection. *J Infect Dis* 2012;206:275-282
- Anthony IC, Bell JE. The neuropathology of HIV/AIDS. *Int Rev Psychiatry* 2008;20:15-24
- Reiche EMV, Morimoto HK, de Almeida ERD, Oliveira SR, Kallaur AP, Simão ANC. *Oxidative stress and human immunodeficiency virus type 1 (HIV-1) infection*. In: Dichi I, Breganó JW, Simão ANC, Cecchini R, eds. *Role of oxidative stress in chronic diseases*. Boca Raton, FL: CRC Press, 2014:45-89
- Barber SC, Shaw PJ. Oxidative stress in ALS: key role in motor neuron injury and therapeutic target. *Free Radic Biol Med* 2010;48:629-641

26. Wang X, Michaelis EK. Selective neuronal vulnerability to oxidative stress in the brain. *Front Aging Neurosci* 2010;2:12
27. Chen Y, An H, Zhu H, Stone T, Smith JK, Hall C, et al. White matter abnormalities revealed by diffusion tensor imaging in non-demented and demented HIV+ patients. *Neuroimage* 2009;47:1154-1162
28. Corrêa DG, Zimmermann N, Doring TM, Wilner NV, Leite SC, Cabral RF, et al. Diffusion tensor MR imaging of white matter integrity in HIV-positive patients with planning deficit. *Neuroradiology* 2015;57:475-482
29. Feldman HM, Yeatman JD, Lee ES, Barde LH, Gaman-Bean S. Diffusion tensor imaging: a review for pediatric researchers and clinicians. *J Dev Behav Pediatr* 2010;31:346-356
30. Stebbins GT, Smith CA, Bartt RE, Kessler HA, Adeyemi OM, Martin E, et al. HIV-associated alterations in normal-appearing white matter: a voxel-wise diffusion tensor imaging study. *J Acquir Immune Defic Syndr* 2007;46:564-573
31. Wu Y, Storey P, Cohen BA, Epstein LG, Edelman RR, Ragin AB. Diffusion alterations in corpus callosum of patients with HIV. *AJNR Am J Neuroradiol* 2006;27:656-660
32. Zhu T, Zhong J, Hu R, Tivarus M, Ekholm S, Harezlak J, et al. Patterns of white matter injury in HIV infection after partial immune reconstitution: a DTI tract-based spatial statistics study. *J Neurovirol* 2013;19:10-23
33. Budde MD, Xie M, Cross AH, Song SK. Axial diffusivity is the primary correlate of axonal injury in the experimental autoimmune encephalomyelitis spinal cord: a quantitative pixelwise analysis. *J Neurosci* 2009;29:2805-2813
34. Shin NY, Hong J, Choi JY, Lee SK, Lim SM, Yoon U. Retrosplenial cortical thinning as a possible major contributor for cognitive impairment in HIV patients. *Eur Radiol* 2017;27:4721-4729
35. Thompson PM, Dutton RA, Hayashi KM, Toga AW, Lopez OL, Aizenstein HJ, et al. Thinning of the cerebral cortex visualized in HIV/AIDS reflects CD4+ T lymphocyte decline. *Proc Natl Acad Sci U S A* 2005;102:15647-15652
36. Stubbe-Drger B, Deppe M, Mohammadi S, Keller SS, Kugel H, Gregor N, et al.; German Competence Network HIV/AIDS. Early microstructural white matter changes in patients with HIV: a diffusion tensor imaging study. *BMC Neurol* 2012;12:23
37. Schmahmann JD, Smith EE, Eichler FS, Filley CM. Cerebral white matter: neuroanatomy, clinical neurology, and neurobehavioral correlates. *Ann N Y Acad Sci* 2008;1142:266-309
38. Turken A, Whitfield-Gabrieli S, Bammer R, Baldo JV, Dronkers NF, Gabrieli JD. Cognitive processing speed and the structure of white matter pathways: convergent evidence from normal variation and lesion studies. *Neuroimage* 2008;42:1032-1044
39. Gutiérrez R, Boison D, Heinemann U, Stoffel W. Decompaction of CNS myelin leads to a reduction of the conduction velocity of action potentials in optic nerve. *Neurosci Lett* 1995;195:93-96
40. Tolhurst DJ, Lewis PR. Effect of myelination on the conduction velocity of optic nerve fibres. *Ophthalmic Physiol Opt* 1992;12:241-243
41. Waxman SG. Determinants of conduction velocity in myelinated nerve fibers. *Muscle Nerve* 1980;3:141-150
42. Wilson TW, Heinrichs-Graham E, Robertson KR, Sandkovsky U, O'Neill J, Knott NL, et al. Functional brain abnormalities during finger-tapping in HIV-infected older adults: a magnetoencephalography study. *J Neuroimmune Pharmacol* 2013;8:965-974
43. Chung SJ, Shin JH, Cho KH, Lee Y, Sohn YH, Seong JK, et al. Subcortical shape analysis of progressive mild cognitive impairment in Parkinson's disease. *Mov Disord* 2017;32:1447-1456
44. Katzen HL, Levin BE, Weiner W. Side and type of motor symptom influence cognition in Parkinson's disease. *Mov Disord* 2006;21:1947-1953
45. Tomer R, Levin BE, Weiner WJ. Side of onset of motor symptoms influences cognition in Parkinson's disease. *Ann Neurol* 1993;34:579-584